Method for independent control of particle size and distance in rhodium epitaxy on TiO$_2$(110)-(1 × 2) surface
An STM study

A. Berkó, F. Solymosi *

Department of Solid State and Radiochemistry,
University of Szeged and Reaction Kinetics Research Group of the Hungarian Academy of Sciences, P.O. Box 168,
H-6701 Szeged, Hungary

Abstract

A method for independent control of the particle size and distance is presented for rhodium epitaxy on TiO$_2$(110)-(1 × 2) surface. The real space imaging of the surface morphology was performed by scanning tunneling microscopy. The amount of the deposited rhodium was checked by Auger electron spectrometry. The method consists of two steps: (i) evaporation of 0.001–0.050 ML equivalent of rhodium at room temperature with a post-annealing at 1100 K ("seeding"); (ii) post-deposition of rhodium for growing of the Rh nanoparticles formed in step (i) ("growing"). The mechanism of this procedure is based on the large difference of the surface diffusion coefficient between Rh adatoms and Rh nanocrystallites larger than 1–2 nm. In the first step the average distance between the metal particles is controlled in the range 5–200 nm, the second step determines the particles size (2–50 nm). This work demonstrates that the diffusion processes of metal nanoparticles of different sizes and the growing modes of the crystallites can be studied in detail by application of seeded surfaces. © 1998 Elsevier Science B.V.

Keywords: Diffusion and migration; Epitaxy; Growth; Metal–insulator interfaces; Nucleation; Rhodium; Scanning tunneling microscopy; Titanium oxide

1. Introduction

The production of regular cluster-assembled materials with independently predetermined particle size, shape and separation is one of the most important aims in the recent nanotechnology research. These materials may have many interesting properties which can be exploited for example in the fields of heterogeneous catalysis, the development of nanoelectronic devices and quantum dots research. The classical route for production of these types of materials is the patterning by lithography technique. The electron beam-induced vapour deposition of individual submicron features, or more recently the nanolithography/deposition performed by scanning probe techniques (such as STM for example) are relatively new methods for this purpose, where the feature size can be as low as 1 nm. This is better by two orders of magnitude than that attainable by the classical lithography route. The main disadvantage of the recent atom probe-induced procedures for industrial applications is the low speed of the manufacturing. This disadvantage can be avoided

* Corresponding author. Fax: (+36) 62 322378.

by ordered nucleation of the nanoparticles in which the thermodynamic properties of the surface diffusion are exploited. More generally, all efforts for exploiting the nanoscale self-organization of the growth processes belong to the topic of material research. From this point of view the periodically stepped or reconstructed surfaces more or less fulfil the demand of inhomogeneous and/or anisotropic surface diffusion properties for different admaterials resulting in ordered nucleation controlled by the substrate, as was already demonstrated in some examples [1–5].

In a recent study [6] we have reported an STM study on the thermal behaviour of rhodium evaporated on the $TiO_2(110)$-(1×2) surface at room temperature. It was found that on the effect of annealing at 1100 K in UHV the rhodium particles isolate clearly from the titania substrate resulting in hexagonal shape crystallites of 3–5 nm diameter with 3–5 atomic layer thick plates with (111) plane parallel to the surface of the support. At very low rhodium deposition, below 2–3% of a monolayer (ML), the average distance of the rhodium particles is varied in the range 5–100 nm as a function of the amount of surface rhodium evaporated at room temperature. At the same time the particle size (average diameter) exhibits only a slight alteration (2–3 nm). Although the surface diffusion coefficient was not determined quantitatively, the experimental results clearly indicate that the surface diffusion coefficient of Rh crystallites depends strongly on the particle size. The mobility of the Rh nanoparticles of 3–4 nm diameter (or larger) is very low at 1100 K, while the individual Rh atoms are mobile even at room temperature.

In this work clear experimental evidence is presented for the possibility of independent control of the size and average distance of the grown rhodium nanocrystallites. It is also demonstrated that the shape and orientation of the particles are influenced by the anisotropic structure of the substrate.

2. Experimental

The experiments were carried out in a UHV chamber equipped with a commercial STM head (WA Technology), a three-grid AES-LEED analyser, a quadrupole gas analyser, an Ar^+ gun and an auxiliary UHV compatible transfer chamber. An ultimate pressure of 5×10^{-8} Pa was attained by an ion-getter pump and a titanium sublimation pump.

The polished $TiO_2(110)$ oriented sample was purchased from Crystal Tec. It was clipped on a Ta plate and mounted on a transferable sample cartridge. An ohmically heated tungsten filament positioned just below the Ta plate served for annealing of the probe. The temperature in the range 300 K–1100 K was checked by a thin chromel–alumel thermocouple attached to the side of the sample. An infrared thermometer for outside temperature controlling was also applied from time to time. The cleaning procedure of the $TiO_2(110)$ surface consisted of a few hours annealing at 800 K in UHV, some cycles of Ar^+ ion bombardment (10 min, 2 kV, 10^{-5} A cm^{-2}) at room temperature and annealing at 1100 K for 10 min in order to produce well ordered 1×2 reconstructed structure [7]. This procedure resulted also in some reduction of the bulk and it increased the conductivity of the probe sufficiently for STM measurements.

Rhodium was deposited by heating of high purity (99.995%) Rh filament at a distance of approximately 20 mm from the sample. The amount and the cleanness of the epitaxial Rh layer on the $TiO_2(110)$-(1×2) surface was checked by Auger electron spectroscopy. The ultra low deposition of the metal (<0.02 ML) undetectable by AES was controlled by duration of the evaporation. The typical deposition rate was 0.1 ML min^{-1}. STM imaging of the surface was performed by a chemically edged tungsten tip sharpened from time to time in situ by applying 5–10 V pulses or by using a continuous positive 40–70 V bias potential at 10 nA tunneling current between the tip and the sample. Tunneling conditions of $+1.5$ V bias and 0.2 nA tunneling current were typically used for STM imaging. The 256×256 points of an image were collected within 1–3 min depending on the size of the crystallites. For better visualization of the surface morphology a commercial software packet (Photopaint) was applied for image processing. The characteristic pictures shown in this work were chosen from a

number of images recorded on the different regions of the same sample. It is worth mentioning that the overall morphology after the different treatments measured for different sample regions proved to be quite similar.

3. Results and discussion

3.1. Seeding and growing of Rh particles

The detailed study of the effects of rhodium deposited on the surface of $TiO_2(110)$-(1×2) and of thermal treatment in UHV was published elsewhere [6]. The main characteristics are summarized as follows.

The deposition of approximately 0.01 ML of rhodium onto well ordered $TiO_2(110)$-(1×2) surface at 300 K results in highly dispersed Rh particles consisting of 6–8 atoms. The average size of the crystallites is approximately 1 nm. A slight increase in the diameter of these Rh nanoparticles was experienced after several hours even at room temperature. The Rh clusters are mainly located on the terraces of titania (no preferred step decoration) and exert no influence on the original (1×2) structure of the titania substrate. With the increase of the rhodium coverage up to 0.1 ML, the average particle size increases from 1 nm to 3 nm accompanied by concealing the original structure of $TiO_2(110)$-(1×2). Above 0.10 ML coverage no significant changes occurred in the surface morphology. Following the annealing of the Rh/TiO_2 system, the encapsulation of the Rh particles in the temperature range 500–700 K, the coalescence of the bumps (formed at room temperature) between 700 and 900 K and the de-encapsulation of the encapsulated Rh crystallites at 1100 K were distinguished.

Fig. 1A and B show the surface morphology of rhodium at two coverages on $TiO_2(110)$-(1×2). The deposition of Rh was carried out at 300 K which was followed by annealing at 1100 K in UHV for 10 min. This procedure is called "seeding". The size of the images is 100 nm × 100 nm, which is the smallest area in these cases representing the characteristic surface structure. Although the average terrace size of the support material is

different in the two cases, the aggregation behaviour of the metal particles, or in other words their size, is not influenced substantially by this property. It means that the surface diffusion of the small Rh nanocrystallites (below 1 nm) or individual Rh atoms are not radically different for the terraces and for the steps oriented in [001]. On both images (A and B) the 1–2 nm particles are localized at the terrace edges and the distribution of the particle size is rather narrow. The basic difference between the two cases is the number of Rh particles appearing per unit area. In the case of the lower Rh coverage (0.003 ML) the average number of Rh crystallites is 3–4 distributed on a 100 nm × 100 nm surface area (marked by circles), whereas at 0.020 ML of Rh this value is approximately 16–18. From this feature we may conclude that the particle density changes almost linearly with the amount of evaporated metal in this low coverage range.

Both surfaces characterized by the images above were exposed further to rhodium of 1 ML equivalent at 1100 K in UHV (Fig. 1C and D). This procedure is called "growing". The first important observation is that the number of particles per unit area, or in other words the average distance between the neighbour particles, did not change by the post-deposition. In the case of 0.003 ML, the average distance is 90–100 nm, while at 0.020 ML it is 30–40 nm. The average diameter of the crystallites varies in the range 6–12 nm and the aspect ratio (diameter/height) between 5 and 10 (higher for larger particles). Totally different morphology can be produced when the sample is exposed forthwith to 1 ML of rhodium at room temperature and annealed subsequently at 1100 K for 10 min in UHV (Fig. 1E). In this case smaller Rh particles (2–3 nm) are formed and distributed rather homogeneously with an average distance of 3–4 nm. It should be pointed out that the further annealing (for some hours) at 1100 K did not cause any change in the surface morphology for all cases discussed above.

On the shape of the particles (shown in Figs. 1C and D) we can distinguish two groups: (i) particles with quasi-isotropic hexagonal shape (in some cases tetragonal) and only slightly (30–50%) elongated in the crystallographic orientation of [001],
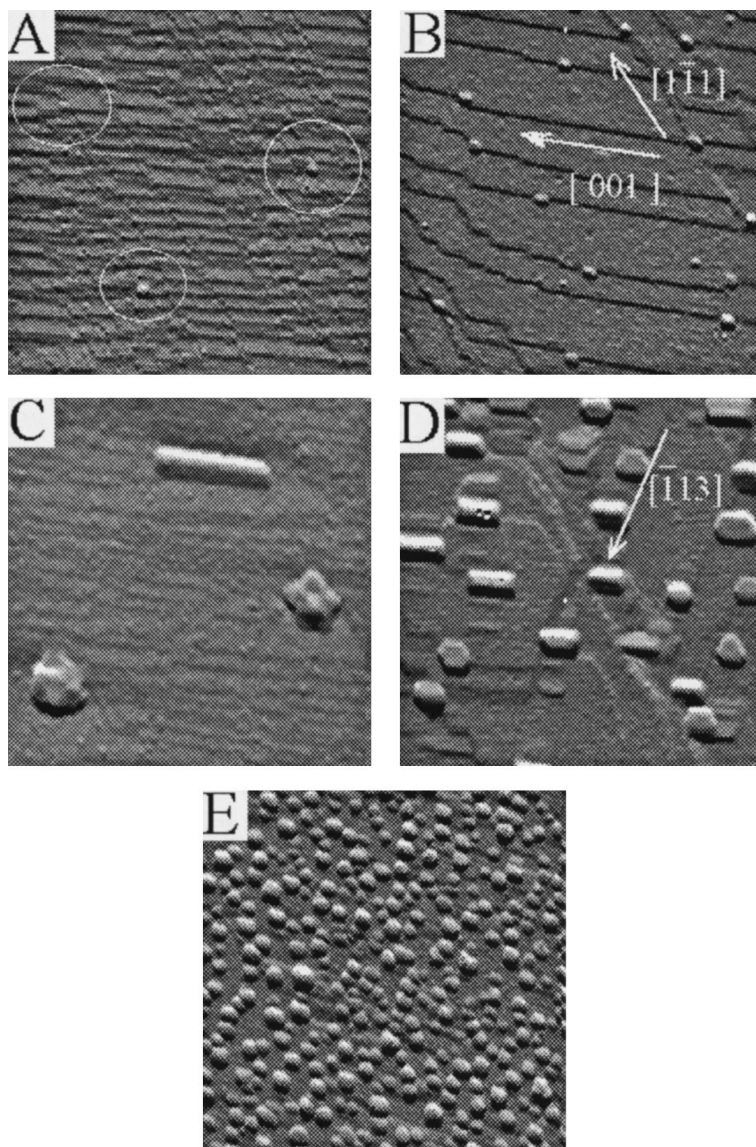
Fig. 1. Control of the average distance of the Rh particles supported on $TiO_2(110)$-(1×2) by the amount of predeposited Rh at 300 K: (A) 0.003 ML of Rh and (B) 0.020 ML of Rh. Both surfaces were annealed at 1100 K. Growing of the Rh crystallites by post-deposition of 1 ML equivalent of rhodium at 1100 K on the seeded surfaces above (C, D). The characteristic morphology of the surface formed after deposition of 1 ML of rhodium at room temperature followed by annealing at 1100 K (E). The image size is 100 nm × 100 nm in all cases.

and (ii) particles with strongly elongated shape in the crystallographic orientation of [001]. The two-dimensional aspect ratio (parallel to the surface plane) for the latter case can be as high as 5–10. The number of Rh crystallites of hexagonal shape was typically 2–3 times higher than that of strongly elongated shape, and this ratio changed only slightly for the different regions of the sample. Two typical examples of the crystallites are shown on a scale of 50 nm × 50 nm in Fig. 2A and B. Unfortunately, due to the low resolution, we could not attain an atomically resolved imaging of the
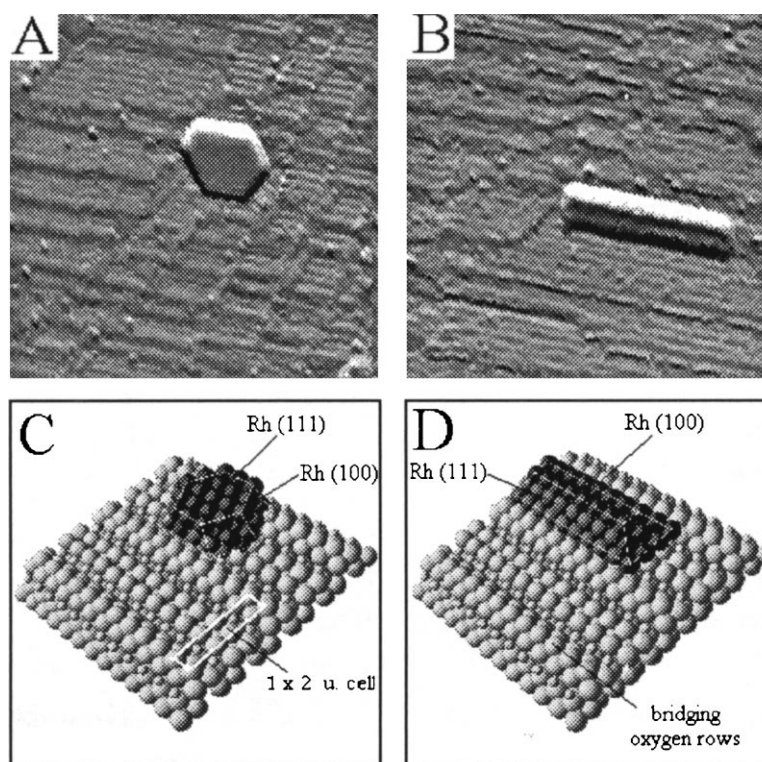
Fig. 2. STM images (A, B) and models (C, D) of the two typical Rh nanoparticles formed by seeding and growing procedure. The size of the STM images is 50 nm × 50 nm.

upper plates of the Rh particles, however, the STM images reveal clearly that the shape of the metal particles formed is influenced by the periodic structure of the substrate: the elongation for all particles is preferred in the [001] orientation (the direction of the bridging oxygen rows). Two explanations can be proposed for this behaviour: (i) the anisotropic surface diffusion of the metal particles on the titania support, and (ii) the different diffusion rates for the Rh crystallite itself with possibly divergent inner structures. If the first assumption is the dominant process, one would expect nearly the same aspect ratio of width–length for all the particles. The 30–50% elongation can be attributed to this effect. At the same time the existence of strongly elongated crystallites supports the second mechanism, which means the formation of innerly different types of crystallites. Taking into account that the most stable planes of the Rh (fcc) crystals are (111) and (100) orientations, we

prefer the existence of two crystallites with different inner structure drawn in Fig. 2C and D. In the case of the hexagonal outline crystallites the top face is (111) plane oriented parallel to the $TiO_2(110)$-(1×2) surface, the side faces are likely (111) and (100) facets. The strongly elongated crystallites consist of (100) top face parallel to the plane of titania support and the side faces are of (111) facets.

In this context we point out that in a study of polycrystalline Rh/TiO_2 catalysts two important conclusions were made [8]: (i) the supported Rh particles selectively interact with the (110) faces of the rutile TiO_2 support; (ii) the Rh particles are forming two kinds of structures: flat platelets and atomic rows along the [001] direction. In a more recent work it was shown that the supported Rh crystallites have preferred orientation to the TiO_2 support facets and also two characteristic types of Rh crystallites were found by high resolution

electron microscopy: (111) or (100) top faced metal particles parallel to the support surface [9]. The conclusions of these studies and the results of the present work reveal that the TiO$_2$(110) surface covered by rhodium is an excellent model system for the simulation of real catalysts, as this planar catalyst shows all the main structural features that were observed for polycrystalline supported Rh/TiO$_2$ catalyst.

Note that similar features were observed when the Rh particles were grown gradually by post-deposition of an increasing amount of Rh at 1100 K in UHV on a surface seeded by 0.003 ML of rhodium. The number of particles distributed per unit area, or in other words the average distance between them, does not change by these treatments. After post-deposition of 0.25 ML the average diameter of the hexagonal Rh particles is approximately 4–5 nm, while for 1 ML this value increases up to 8–10 nm.

3.2. Characterization of the surface diffusion of Rh particles

In this section the diffusion ability of Rh crystallites of different sizes is investigated in the temperature range 700–1100 K. This is the temperature range where the diffusion of the small Rh clusters exhibits significant deviations at different surface sites like terraces, steps and crosspoints of steps. The aim of these experiments was to visualize the free path and site sensitivity of the diffusion of Rh atoms or small clusters as a function of temperature of the substrate.

The TiO$_2$(110)-(1 × 2) surface was exposed to 0.003 ML of Rh at room temperature and annealed at 1100 K in UHV for 10 min. The characteristic surface structures formed after the seeding can be seen in Figs. 3A and 4A with image sizes of 50 nm × 50 nm and 100 nm × 100 nm, respectively. The latter area is sufficiently large for characterization of the total surface: it shows that on average 4–5 particles are distributed randomly on a 100 nm × 100 nm area and that the crystallites are preferentially localized at the crosspoints of steps oriented in [001], [1$\bar{1}$1] and [$\bar{1}$13] directions. The extended annealing of a few hours does not cause any change of the average distance between the

particles. This fact suggests that the Rh crystallites of a few atoms are most strongly bonded to these types of surface sites, and they are not mobile at 1100 K. In the following experimental series this surface was exposed to 0.02 ML doses of Rh at stepwisely decreasing temperatures (Fig. 4B–J). After the exposure of the metal at 1100 K, 1050 K and 1000 K there is no sign of formation of new particles, only the existing Rh crystallites are growing further (Fig. 3B–D). Accordingly the Rh atoms are sufficiently mobile in this temperature range, and they are trapped on the existing particles but not trapped on any site of the support. The highest temperature where smaller crystallites appear is 950 K (Fig. 3E). The new crystallites are bonded to the crosspoints of the different steps and they do not accumulate on the terraces or [001] steps. This is clearly seen in Fig. 3F. In contrast to this behaviour, the small protrusions appearing both on the terraces and the terrace edges after deposition at 850 K suggest clearly that the diffusion of small Rh crystallites is already terminated at this temperature, preventing their trapping or agglomerization. Obviously, the same was observed at lower temperatures (Fig. 3G–J). It is important to note that no temperature regime was found where the capturing at the [001] steps would be preferred against the trapping at the terraces, in other words the mobility of the Rh atoms or smaller crystallites (<1 nm) is not basically different on these sites. The texture of the surface pretreated in the way described above can be seen on a scale of 100 nm × 100 nm in Fig. 4B. The ordering of the new smaller crystallites in the direction of [$\bar{1}$13] and the larger ones formed in the seeding process and distributed randomly can be clearly distinguished.

In order to examine the mobility of somewhat larger Rh particles, the surface was annealed for 10 min in UHV at 900 K and 1100 K (Fig. 3K and L). Annealing at 900 K causes only a slight change in the morphology of the pretreated surface, showing that the Rh crystallites of 2–3 nm are not mobile at this temperature even when they are localized on the terraces (Fig. 3K). The annealing at 1100 K, however, results in the agglomerization of the 2–3 nm particles bonded to the terraces and [001] steps (Fig. 3L). At the same time the particles
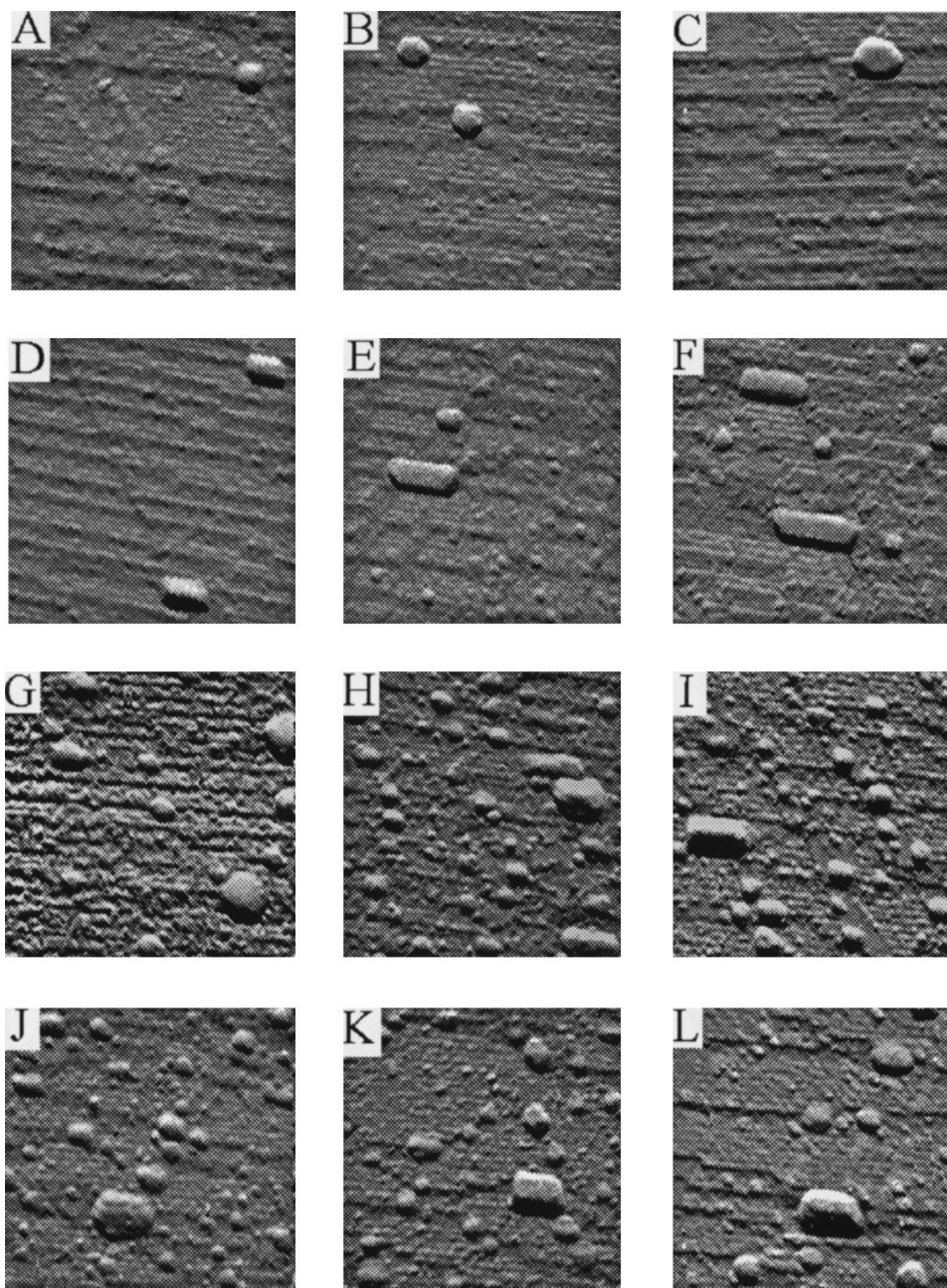
Fig. 3. Effects of subsequent post-deposition of 0.02 ML of Rh at decreasing temperatures in the range 1100 and 700 K on a seeded (0.003 ML of Rh) TiO$_2$(110)-(1×2) surface. After seeding (A) and subsequent deposition of 0.02 ML of Rh at 1100 K (B), 1050 K (C), 1000 K (D), 950 K (E), 900 K (F), 850 K (G), 800 K (H), 750 K (I) and 700 K (J). Effects of subsequent annealing at 900 K (K) and 1100 K (L) in UHV for 10 min. The size of the images is 50 nm × 50 nm.
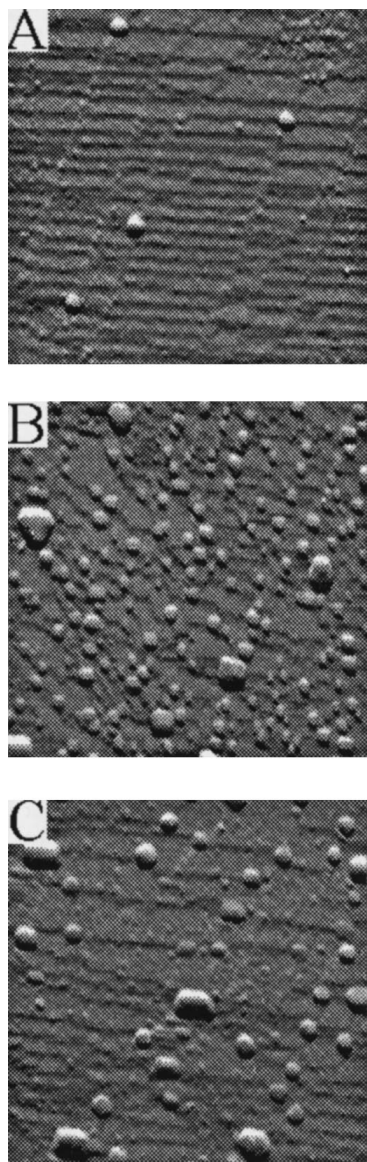
Fig. 4. Larger scale images (100 nm × 100 nm) after the treatments presented in Fig. 3 (see text).

with diameter of 3–4 nm and localized at [001] steps are not mobile even at this high temperature. This situation is imaged on a larger scale (100 nm × 100 nm) in Fig. 4C.

The study of further details of the diffusion of Rh atoms on different sites of the titania surface (such as terraces, steps or vacancies) requires low temperature (< 300 K) measure-

ments. Nevertheless, our results clearly show that nucleation and sticking of small particles vary with the special sites of the surface as well as with the size of the Rh crystallites. This behaviour is obviously connected to the local oxidation state of the titania support. At the crosspoint of two different steps there are certainly Ti ions in a more reduced state (such as Ti^{2+} or Ti^{3+}) which donate electrons to the Rh atoms or clusters. As a result the admetal particles are most strongly bonded on these sites. The method presented here makes it possible to decorate certain sites preferentially and to study the lateral dependence of the electron transfer to the admetal particles.

4. Conclusions

The deposition of rhodium on $TiO_2(110)$-(1×2) surface at different temperatures delivered important information about the diffusion of supported Rh nanoparticles. The very small particles of Rh (< 1 nm) are very mobile above 900 K and only at the surface sites of the crosspoint of [001], [$1\bar{1}1$] and [$\bar{1}13$] steps can be captured with higher probability. Below 900 K, their mobility decreases drastically both on the terraces and on the step regions. The larger Rh nanoparticles with a diameter of 1–3 nm are bonded strongly and diffuse very slowly even at 1100 K. The Rh crystallites larger than 3 nm are practically immobile even at this high temperature. Following the evaporation of Rh at approximately 900 K, the step lines of [$\bar{1}13$] and [$1\bar{1}1$] can be preferentially decorated. The large difference of the surface diffusion coefficient for individual Rh atoms and Rh particles larger than 1 nm can be exploited for growing giant Rh particles with predetermined size and average distance on the $TiO_2(110)$-(1×2) surface. The applicability of this specially grown supported planar catalyst is demonstrated in a recent work from our laboratory [10].

References

[1] H. Hofmeister, S. Grosse, G. Gerth, H. Haefke, Nanostruct. Mater. 6 (1995) 529.

[2] T.L. Morkved, P. Wiltzius, H.M. Jaeger, D. Grier, T.A. Witten, Appl. Phys. Lett. 64 (1994) 422.

[3] D.D. Chambliss, R.J. Wilson, S. Chiang, Phys. Rev. Lett. 66 (1991) 1721.

[4] G.M. Francis, L. Kuipers, J.R.A. Cleaver, R.E. Palmer, J. Appl. Phys. 79 (6) (1996) 2942.

[5] H. Hofmeister, S. Grosse, G. Gerth, H. Haefke, Phys. Rev. B 49 (11) (1994) 7646.

[6] A. Berkó, G. Ménesi, F. Solymosi, Surf. Sci. 372 (1997) 202.

[7] A. Berkó, F. Solymosi, Langmuir 12 (1996) 1257.

[8] S. Fuentes, A. Vázauez, J.G. Pérez, M.J. Yacamán, J. Catal. 99 (1986) 492.

[9] S. Bernal, F.J. Botana, J.J. Calvino, C. López, J.A. Pérez-Omil, J.M. Rodriguez-Izquierdo, J. Chem. Soc., Faraday Trans. 92 (15) (1996) 2799.

[10] A. Berkó, I. Ulrych, K. Prince, F. Solymosi, J. Phys. Chem. B, in press.